Rotating Power Electronics for Electrical Machines and Drives - Design Considerations and Examples

Jonas Kristiansen Nøland[1*] and Marta Molinas[2]
[1] Department of Electric Power Engineering, Norwegian University of Science and Technology, Trondheim, Norway
[2] Department of Engineering Cybernetics, Norwegian University of Science and Technology, Trondheim, Norway
[*]E-mail: jonas.k.noland@ntnu.no

***Abstract*—The industrial shift towards rotating power electronics (RPE) promotes brushless flexible rotor excitation, as well as battery-less rotor instrumentation and measurement devices for electrical machines. Recently, the high-power thyristor converter has been proven to be excellent for rotating applications. Moreover, MOSFET components have been successful for low-power rotating applications. However, the question arises whether IGBT's, capacitors and related components are able to withstand the centrifugal forces that are generated due to shaft rotation. In fact, the manufacturers do not conventionally test their power electronic components against cyclic accelerational forces. Moreover, the insulation material in some types of semiconductor modules are viscous and will be affected by rotational forces. This paper addresses the current design challenges and presents new design criteria for RPE systems and applications. Finally, this paper reviews the current technology status for RPE concepts.**

***Index Terms*—Rotating power electronics (RPE), monitoring, measurement, internal processes, rotating rectifiers, thyristor rectifers, IGBT converter, rotating capacitor, rotating chopper, rotor field excitation, brushless electrical machines.**

I. Introduction

Rotating power electronics (RPE) is not something completely new in the application of electrical machines. The passive rotating diode-bridge rectifier has been in operation in the brushless excitation system for synchronous machines since the 1960s [1].

However, the trend towards active rotating power electronics has started. Recently, self-actuated insulated gate bipolar transistors (IGBTs) have been applied to conventional brushless exciter for fast field-flux de-regulation of synchronous machines [2]–[6]. Moreover, active rectification via the thyristor bridge has been applied on the rotating shaft on commercial brushless exciters [7], [8]. Nowadays, extensive research efforts have been made for advances beyond the state-of-the-art [9]–[14].

Similarly, the brushless doubly-fed induction generator (B-DFIG) has been the focus for advancements on variable speed offshore wind power applications [15]–[26]. In automotive applications, a rotating dc-dc converter with MOSFETs has been tested [27]. In classical motor drives, an inverter-integrated rotor has been proposed [28], [29].

The common trend, nowadays, is that RPE continues to be proposed for the replacement of carbon brushes and slip rings for excitation purposes. It is even used to reduce the current needed through the brushes or other mechanical contacts [27]. The possibility for active RPE on the shaft of rotating electrical machines is a direct consequence of the recent developments in reliable wireless communication [30]. Typical communication interfaces are Bluetooth or ZigBee.

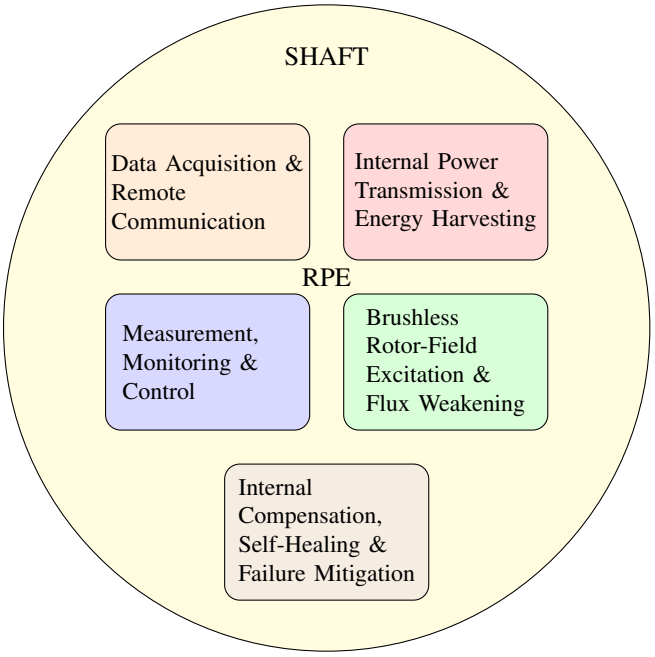

Fig. 1. Outline of systems integrated in a rotating power electronics based drive system for electrical machines

RPE has been evolving for several applications and as a result of development in the high-performance wireless communication interfaces [30] and the implementation of wireless data transmission systems for active rotor monitoring of electrical machines [31].

The IGBT converter has been placed on the generator shaft for the RPE brushless DFIG (RPE-BDFIG) [16]. Maintenance is a major issue which has the main driver towards RPEs. This applies both to land-based power production but especially for offshore installations where replacements of slip rings and carbon brushes are costly.

Fig. 1 highlights five different areas where RPE has growing interests, including brushless and exciter-less excitation systems, energy harvesting for battery-less measurement systems, internal compensation systems for failure mitigation, and data acquisition and remote communication.

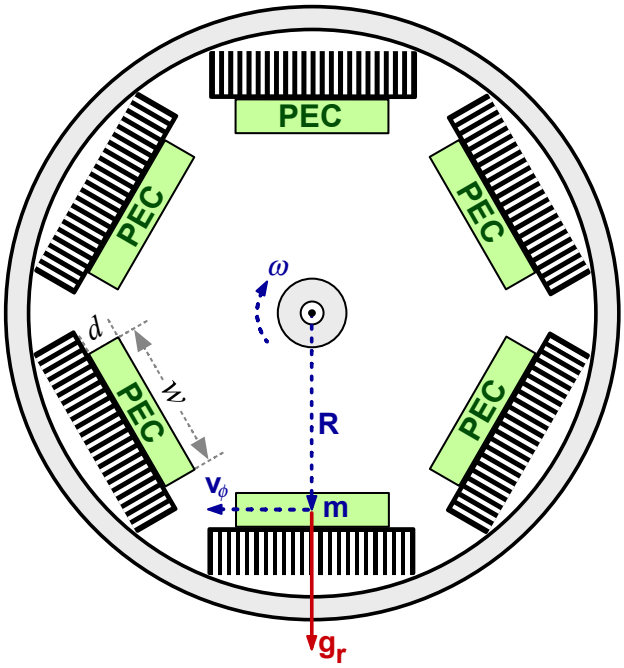

Fig. 2. Two-dimensional view of the power electronics enclosure box including individual switches. See Fig. 4 for a detailed look at the PEC.

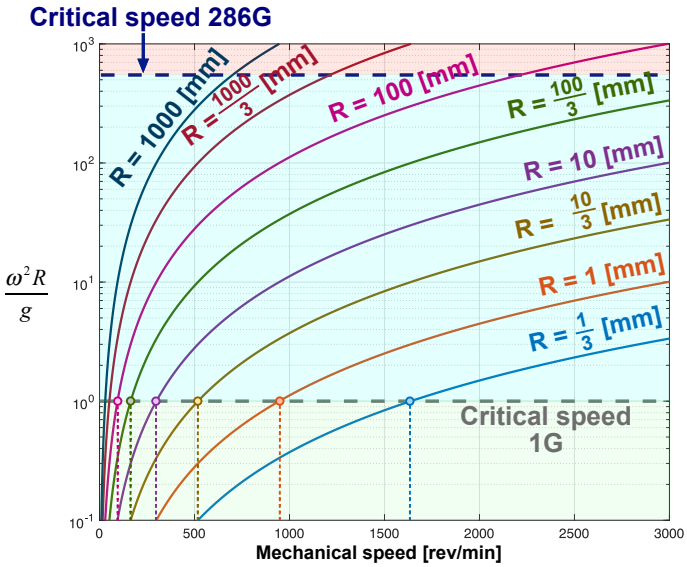

Fig. 3. Normalized acceleration G-force for different rotational radiuses as a function of mechanical speed ($g = 9.81m/s^2$). 1-G and 286-G are highlighted.

The remainder of the paper is organized as follows. Section II presents the proposed mechanical design framework for RPE. Some calculations are visualized to illustrate the implications of different specifications. Then, Section III describes more, in general, the development of RPE and its applications. Finally, Section IV concludes the paper.

II. Mechanical Design Framework for RPE

Power electronics that are attached to the rotor shaft of electrical machines will rotate at nominal speed. As a result, critical components are rotating, and they are subjected to cyclic acceleration loading. The RPE requires better mechanical enclosures as compared with standard components. An enclosure box should hold the RPE components fixed, and it will act with a radial force on the components towards the centre of the shaft. This is similar to power electronics installed in electric vehicles which periodically will be subjected to g-forces and vibrations. This section focuses on formulating an analytical framework for the analysis of forces and stresses (or pressures) acting on RPEs.

A. The centripetal force

The centripetal force that acts on any rotating component is

$$F_r = m\frac{v_\phi^2}{R} = m\omega^2 R, \tag{1}$$

where v_ϕ is the tangential velocity, m is the mass of the component, ω is the mechanical speed (in radians per second), and R is the radial rotating position of the centre of mass of the component with respect to the rotational axis. Notice that if the rotational speed is doubled, the centripetal force will quadruple. The classical setup is illustrated in Fig. 2.

B. The acceleration G-force

According to the equivalence principle, the centrifugal forces have the same physical effect on the mass as gravity ($F_z = mg$). Radial G-forces act as an artificial gravity since inertial forces mimic the effect of gravity. A sustained normal force will act on any mass in order to realize rotation, which is equivalent to a constant change of speed direction. Therefore, it would be meaningful to normalize the centrifugal force with its gravitational force, yielding

$$G_r = \frac{F_r}{F_z} = \frac{\omega^2 R}{g} = \frac{g_r}{g}, \tag{2}$$

where g is the gravitational acceleration $9.81m/s^2$ and G_r quantifies the ratio of the centripetal force with respect to gravity. The gravitational constant of the rotary motion is then given by

$$g_r = \omega^2 R, \tag{3}$$

where g_r is the acceleration of the rotating component. Please recognize that the normalized force is not dependent on the mass itself, only on the mechanical speed and the radius of rotation. The radial g-force is equal to axial G-force when

$$g_r = \omega^2 R = g. \tag{4}$$

It may be useful to calculate the critical speed where the centripetal force is equal to the gravitational force, yielding

$$\omega_{crit} = \sqrt{\frac{g}{R}}. \tag{5}$$

Notice that the critical speed reduces as the radius of rotating increase. If gravity is given as the maximum allowed radial G-force, then

$$R_{crit} = \frac{g}{\omega^2}, \tag{6}$$

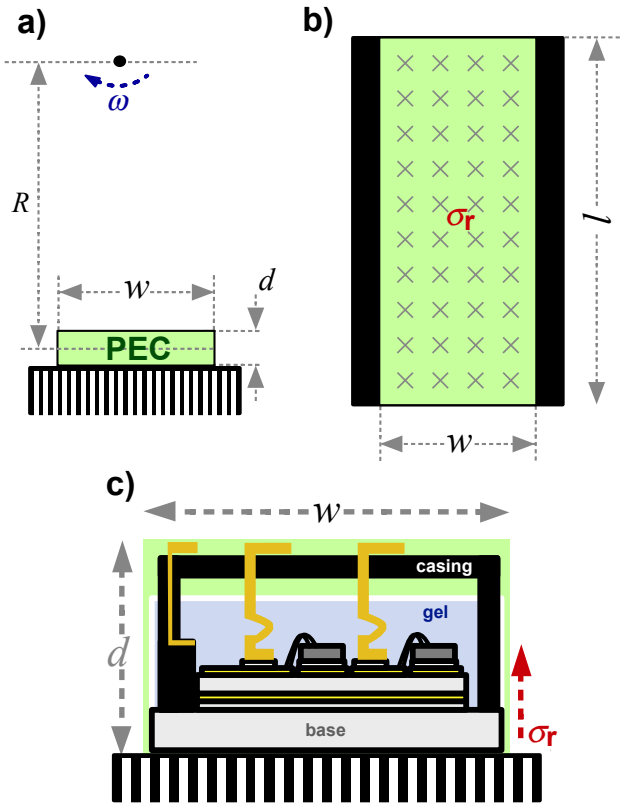

Fig. 4. A detailed look at an IGBT emulating the PEC shown in Fig. 2.

which ultimately will limit the size of the power electronic box. If $n = 500\,\mathrm{r/min}$ and $\omega = 52.36\,\mathrm{rad/s}$, then $R_{crit} = 3.6\,\mathrm{mm}$, which is extremely low considering the diameter of the shaft. However, IGBT components have been strength tested for G-forces up to 286, without deterioration after 33000 repeated cycles [21], which yields $R_{crit} = 1000\,\mathrm{mm}$ for the same rotational speed. A worked example is provided in Section II-E. Fig. 3 illustrates the normalized G-force with respect to rotational radius as a function of the mechanical speed with logarithmic scale.

C. Artificial weight

At critical speed, the components are subjected to equivalent radial G-forces that are continuously changing direction. Rotation around a vertical axis generates a radial G-force perpendicular to the gravitational force. However, rotating around a horizontal axis generates pulsating G-forces since the centripetal force periodically coincides with the direction of gravity. However, for high radial g-forces, the effect of the gravitational force will be negligible. Physically, the centrifugal force acts as an extra weight (or artificial weight) pushing the rotating mass toward the outer boundary. The centrifugal weight is given by

$$m_r = mG_r = \frac{m\omega^2 R}{g}, \tag{7}$$

where mass m_r is an extra mass added to mass m. The stress from m_r depends on the dominance of the centripetal force. In order to account for the distribution of the mechanical stress at the outer boundary, the normal average stress is

$$\sigma_R = \frac{F_r}{A} = \frac{m\omega^2 R}{wl}, \tag{8}$$

in force per cross-sectional area of the RPE component.

D. Internal centrigugal stress

Each RPE component has an axial length l, a radial height d and a tangential width w. The mass of the component is then given by

$$m = \rho V = \rho dwl, \tag{9}$$

or

$$\rho = \frac{m}{V} = \frac{m}{dwl}. \tag{10}$$

Inserting (9) into (8), yields

$$\sigma_R = \rho d\omega^2 R, \tag{11}$$

where the mechanical stress is proportional to the mass density and the thickness of the RPE (in the radial direction). It is important to notice that this is at the outer boundary, where the RPE is supported by the heat sink (indicated in Fig. 2).

The radial stress changes inside the RPE, starting from zero at the inner boundary. The mechanical stress as a function of radius equals

$$\sigma_r(r) = \rho\omega^2 \int_{R-\frac{d}{2}}^{r} r \cdot dr, \tag{12}$$

where each incremental contribution of centrifugal mass is added. The solution to eq. (12) is

$$\sigma_r(r) = \frac{1}{2}\rho\omega^2 \left(r^2 - \left[R - \frac{d}{2} \right]^2 \right). \tag{13}$$

where the radial stress at the outer boundary is

$$\sigma_r \left(R + \frac{d}{2} \right) = \sigma_R, \tag{14}$$

as already derived in eq. (11). Eq. (13) can be normalized with the stress at the outer boundary, yielding

$$\frac{\sigma_r(r)}{\sigma_R} = \frac{r^2}{2dR} - \frac{\left(R - \frac{d}{2}\right)^2}{2dR}, \tag{15}$$

where

$$\frac{\sigma_r \left(R + \frac{d}{2} \right)}{\sigma_R} = 1. \tag{16}$$

When defining a normalized radial position

$$\hat{r} = \frac{r - \left(R - \frac{d}{2} \right)}{d}, \tag{17}$$

the solution to eq. (13) becomes

$$\frac{\sigma_r(\hat{r})}{\sigma_R} = \left(1 - \frac{1}{2}\frac{d}{R} \right) \hat{r} + \frac{1}{2}\frac{d}{R}\hat{r}^2. \tag{18}$$

Notice that the g-force increases linearly towards the outer wheel if the height d is significantly small compared with R.

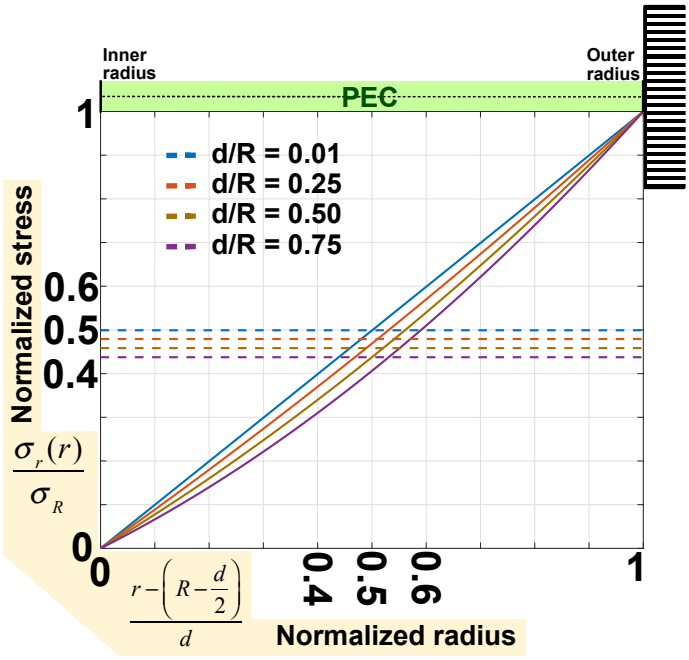

Fig. 5. Normalized internal stress in rotating PEC as a function of the normalized radius. Comparison with the average value for different d/R ratios.

The mean stress inside the rotating PEC is approximately half of the stress at the outer boundary, as illustrated in Fig. 5.

$$\left(\frac{\sigma_r(\hat{r})}{\sigma_R}\right)_{avg} = \frac{1}{2} - \frac{1}{12}\frac{d}{R} \approx \frac{1}{2} \tag{19}$$

E. Worked example

A worked example is presented in Fig. 6 (enclosure box of Fig. 7) with calculations outlined in Table I.

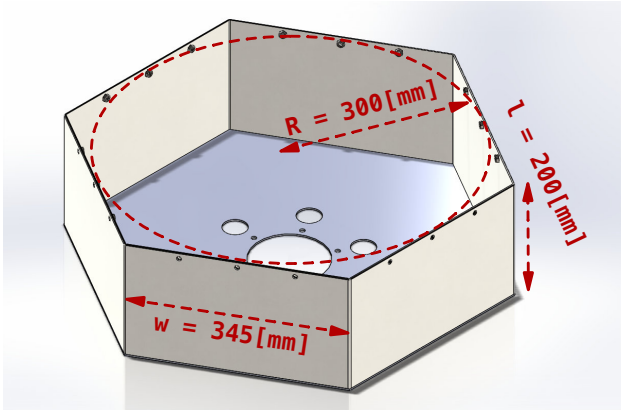

Fig. 6. Example of a built enclosure box (Courtesy of Uppsala University).

III. Challenges and Applications of RPE

The diode bridge rectifier is well-known for its capability to withstand high gravitational forces due to rotation. Nowadays, thyristors have been commercially demonstrated for RPE as well. By employing a similar type of mechanical packaging for IGBTs, IGBTs will become mature for new applications, such as RPE.

TABLE I
Evaluation of Constructed Example

F_r/F_z-ratio	G_r	83.84	G
Critical speed (1G)	$n_{crit,1G}$	54.61	rpm
Nominal mechanical speed	n	500.00	rpm
Critical speed (286G)	$n_{crit,286G}$	923.48	rpm
Critical radius (1G)	$R_{crit,1G}$	3.58	mm
Actual radius	R	300.00	mm
Critical radius (286G)	$R_{crit,286G}$	1023.38	mm

Driven by the need for more robust solutions, more and more commercialized RPE products will appear on the market during the next decade. Until recently, the rotating thyristor bridge has been the only commercialized high-power RPE solution, but very soon, new configurations are expected to take over for many applications. The remainder of the section focuses on some of the current technology challenges.

A. From Bond-Wire to Press-pack IGBTs

Device packaging plays a critical role in RPE systems. In particular, the traditional design of IGBTs with bonding wires and solder layers are highly susceptible to thermo-mechanical stress, with failure as a consequence [32], [33]. New solderless designs employ press-pack or press-fit housing, which was first introduced for thyristors and diodes, and with proven reliability and robustness.

The rotating RPE environment is similar in characteristics with the liquid pressurized environment under the sea. The centrifugal force originates a need for pressure tolerant power electronics, which has similar challenges [34], [35]. Mechanically, the pressure is equivalent to stress. The viscous properties of aluminum oxide (Al_2O_3) [36] is directly subjected to the gravitational forces acting on the module. In fact, the layer of aluminum oxide is the main insulation layer of the IGBTs. Thermal grease is made of Al_2O_3 as well.

The most critical components for IGBT-based RPE topologies would be 1) IGBT modules, 2) IGBT drivers and 3) DC-link capacitors.

B. Strength testing

Mechanical strength has been a focus for high-vibration automotive environments. Components are tested according to international standard 60028-2-6, should be able to withstand vibration stresses of $98\,\mathrm{m/s^2}$ in acceleration amplitude, and shock or impact stresses of $490\,\mathrm{m/s^2}$ with $11\,\mathrm{ms}$ pulsed duration [37], [38]. The intention of the testing is based on the vibrations related to electrical machinery. So far, no test standards have been developed for RPE applications, even though strength tests have been carried out [21]. For RPE applications, the components are placed in rotating enclosure boxes with an inner wheel and an outer wheel surface. The predictions on the RPE fatigue strength is presented in [21].

For wind applications the expected startup intervals per year is about 1100 times.

C. Power capacitors for RPE

Capacitors in RPE-systems are constantly subjected to rotary motion and frequent vibrations. The conventional capacitors, such as Aluminum electrolytic capacitors (Al-Caps), include Al_2O_3, which are high in energy density. However, aluminium oxide is a viscous medium which should be avoided in RPE applications. In addition, it has a relatively high ESR and low current ripple rating. The solid box-type metalized polypropylene film capacitors (MPPF-Caps) has become the popular choice for medium and high power applications, such as electric vehicles [39]. Its capability of overcoming internal defects are unique and susceptibility against cracks. In addition, it has benefits of space savings, or high volumetric efficiency, when comparing it to other technologies. The box-type MPPT-Caps include vibration tolerance under severe vibration-regimes and harsh industrial applications when comparing it to the standard dipped-film capacitors.

Fig. 6 includes an enclosure box with thin-film capacitors included.

D. Additional considerations

The design of rotating enclosure boxes for RPE has been covered in recent contributions [22], [43] (see Figs. 6 and 7). The main issues with the construction of a rotating assembly are mechanical stability and system reliability. The most straightforward choice is to design the system with controllers on both rotating and stationary frames, with a wireless communication interface in between. In fact, direct transmission of PWM signals over the wireless link would reduce the system performance with respect to bandwidth and reliability.

The rating of the RPE depends on the application. For synchronous machines, the losses in the field winding are less than $1\,\%$ of its rated capacity. In large generators the losses are actually less than $0.35\,\%$. Typically, the field winding is highly inductive and with low resistance. The field current is large, but the field voltage is low. Extra capability is needed for ceiling voltage and/or ceiling current operation.

The application of brushless DFIG should typically be designed with hight ratings. Normally, the variable-speed operation requires a slip-power of about $25\,\%$ of the rated capacity of the DFIG. Moreover, the RPE is a back-to-back topology with a high amount of switching devices compared with the field-excitation of synchronous machines.

IV. Discussion and Conclusion

This paper has highlighted the ongoing developments going on in the area of rotating power electronics for electrical machines, drives and related systems. Moreover, the paper provides a new framework for design and stress analysis of rotating power electronic (RPE) components placed in rotating enclosure boxes. A worked example is highlighted.

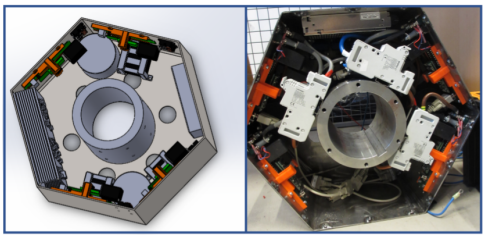

Fig. 7. Example of enclosure box with RPE, measurements and wireless controller [43] (Courtesy of Uppsala University). **Left:** CAD-drawing. **Right:** Final assembly.

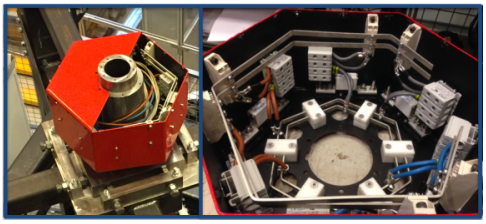

Fig. 8. Rotating thyristor rectifier box on synchronous generator test rig at Uppsala University (Courtesy of Uppsala University). **Left:** On test bench. **Right:** Inside view.

Different RPE technical solutions and applications have been discussed throughout the paper. In addition, Table II summarizes the main highlights in the literature and the industry regarding RPE based systems for high-end electrical machines. In fact, there are many opportunities for breakthroughs in this field for future innovations. This is just a brief introduction to the myriad of opportunities.

References

[1] T. L. Dillman, F. W. Keay, C. Raczkowski, J. W. Skooglund, and W. H. South, "Brushless excitation," *IEEE Spectrum*, vol. 9, no. 3, pp. 58–66, March 1972.

[2] C. A. Platero, M. Redondo, F. Blázquez, and P. Frías, "High-speed de-excitation system for brushless synchronous machines," *IET Elect. Power Appl.*, vol. 6, no. 3, pp. 156–161, March 2012.

[3] C. A. Platero, F. Blázquez, E. Rebollo, F. R. Blánquez, J. A. Martínez, and M. Redondo, "Enhancement of a high speed de-excitation system for brushless synchronous machines by large blocking voltage semiconductors," in *Proc. IEEE Int. Symp. Diagnost. Electr. Mach. Power Electron. Drives*, Sept 2015, pp. 50–55.

[4] E. Rebollo, F. R. Blanquez, C. A. Platero, F. Blazquez, and M. Redondo, "Improved high-speed de-excitation system for brushless synchronous machines tested on a 20 mva hydro-generator," *IET Elect. Power Appl.*, vol. 9, no. 6, pp. 405–411, 2015.

[5] E. Rebollo, C. A. Platero, F. Blazquez, and R. Granizo, "Internal sudden short-circuit response of a new hsbds for brushless synchronous machines tested on a 15 mva generator," *IET Elect. Power Appl.*, vol. 11, no. 4, pp. 495–503, 2017.

[6] C. A. P. Gaona, F. B. García, P. F. Marín, M. R. Cuevas, R. G. Arrabé, and C. C. López, "Rapid de-excitation system for synchronous machines with indirect excitation," Feb. 11 2010, US Patent App. 13/201,971.

[7] G. Shrestha, D. Tremelling, W. Arshad, W. Ouyang, and J. Westerlund, "Systems and methods concerning exciterless synchronous machines," Jan. 16 2015, US Patent App. 14/598,926.

[8] E. Silander, "Rotating electrical machine," Apr. 26 2016, US Patent App. 9/325,225.

[9] J. K. Nøland, K. B. Hjelmervik, and U. Lundin, "Comparison of thyristor-controlled rectification topologies for a six-phase rotating brushless permanent magnet exciter," *IEEE Trans. Energy Convers.*, vol. 31, no. 1, pp. 314–322, March 2016.

TABLE II
EXAMPLES OF ROTATING PECS FOR DIFFERENT APPLICATIONS

PEC type	*Technical solution*	*Application*	*Reference*
Diodes (only)	• Brushless excitation systems for synchronous machines ;	• Small-to-medium classical power generation;	[40], [41]
Thyristors (only)	• High-speed response brushless excitation systems;	• Large power generation (e.g Hydropower)	[42]
MOSFETs	• High-frequency buck converter for field excitation ;	• Automotive alternators;	[27]
	• Boost converter for harmonic excitation	• Exciter-less marine propulsion motors	[7]
	• Inverter integrated rotor for field excitation	• Self-excited wound-rotor synchronous motors	[28], [29]
	• Boost converter and rectifier for energy harvesting	• Rotor instrumentation in electrical machines	[31]
IGBTs	• Brushless excitation of doubly-fed induction generators;	• Offshore wind power generation;	[16]
	• High-speed brushless de-excitation system;	• Medium-size power generation (e.g. Hydropower);	[2]

[10] J. K. Nøland, F. Evestedt, J. J. Pérez-Loya, J. Abrahamsson, and U. Lundin, "Evaluation of different power electronic interfaces for control of a rotating brushless PM exciter," in *Proc. Ann. Conf. IEEE Ind. Electron. Soc.*, Oct 2016, pp. 1924–1929.

[11] ——, "Design and characterization of a rotating brushless outer pole PM exciter for a synchronous generator," *IEEE Trans. Ind. Appl.*, vol. 53, no. 3, pp. 2016–2027, May 2017.

[12] ——, "Comparison of thyristor rectifier configurations for a six-phase rotating brushless outer pole PM exciter," *IEEE Trans. Ind. Electron.*, vol. 65, no. 2, pp. 968–976, Feb 2018.

[13] J. K. Nøland, F. Evestedt, J. J. Perez-Loya, J. Abrahamsson, and U. Lundin, "Testing of active rectification topologies on a six-phase rotating brushless outer pole pm exciter," *IEEE Trans. Energy Convers.*, vol. 33, no. 1, pp. 59–67, March 2018.

[14] J. K. Nøland, "A New Paradigm for Large Brushless Hydrogenerators: Advantages Beyond the Static System," Ph.D. dissertation, Digital Comprehensive Summaries Uppsala Dissertations of the Faculty of Science and Technology 1491, Acta Universitatis Upsaliensis, 2017.

[15] N. u. R. Malik and I. Husain, "Transient and steady-state 3-D electro-thermal design and analysis of the rotating power electronic igbt converter," in *Proc. IEEE Int. Elect. Mach. Drives Conf.*, May 2015, pp. 1342–1347.

[16] I. Husain *et al.*, "Dynamic and steady-state 3-D thermal design and investigation of the rotating power electronic IGBT converter," *IEEE J. Emerg. Sel. Top. Power Electron.*, vol. 4, no. 2, pp. 679–688, 2016.

[17] N. u. R. Malik and C. Sadarangani, "Dynamic modeling and control of a brushless doubly-fed induction generator with a rotating power electronic converter," in *Proc. Int. Conf. Elect. Mach.*, Sept 2012, pp. 900–906.

[18] N. u. R. Malik, C. Sadarangani, and A. Cosic, "Synchronous operation of a rotating power electronic brushless doubly-fed generator," in *Proc. IEEE Ann. Conf. Ind. Electron. Soc.*, Nov 2015, pp. 000 250–000 255.

[19] N. Kusuno, M. Hori, D. Kawamura, D. Satoh, and M. Kimura, "Investigations into optimum design rules for new brushless doubly-fed induction generator: Rotary converter generation system I," in *Proc. Int. Conf. Elect. Mach.*, Sept 2014, pp. 1730–1735.

[20] D. Satoh, N. Kusuno, M. Hori, D. Kawamura, and M. Kimura, "Thermal feasibility study of new type of brushless doubly-fed induction generator: Rotary converter generation system II," in *Proc. Int. Conf. Elect. Mach.*, Sept 2014, pp. 2193–2198.

[21] D. Kawamura, S. Sekine, N. Kusuno, M. Hori, D. Satoh, and M. Kimura, "Fatigue strength prediction of power module for new type of brushless doubly-fed induction generator: Rotary converter generation system III," in *Proc. Int. Conf. on Elect. Mach.*, Sept 2014, pp. 1724–1729.

[22] A. Cosic, Y. Yao, C. Sadarangani, and N. U. R. Malik, "Construction of a rotating power electronic converter for induction machine operation," in *Proc. Int. Conf. Elect. Mach. Syst.*, Oct 2015, pp. 507–511.

[23] Y. Yao, A. Cosic, and C. Sadarangani, "Analysis of an induction machine using a rotor integrated converter with a floating capacitor," in *Proc. Int. Conf. Elect. Mach. Syst.*, Oct 2015, pp. 1851–1857.

[24] Y. Yao and C. Sadarangani, "Optimum operating point of an induction machine using a rotor integrated converter with a floating capacitor," in *Proc. IEEE Int. Power Electron. Motion Contr. Conf.*, May 2016, pp. 98–103.

[25] N. u. R. Malik, C. Sadarangani, and M. Lindmark, "Theoretical and experimental investigation of the self-excited rotating power electronic induction machine," in *Proc. Ann. Conf. IEEE Ind. Electron. Soc.*, Nov 2011, pp. 2048–2053.

[26] N. u. R. Malik, C. Sadarangani, A. Cosic, and M. Lindmark, "Induction machine at unity power factor with rotating power electronic converter," in *Proc. Int. Symp. Power Electron. Elect. Drives Aut. Mot.*, June 2012, pp. 401–408.

[27] L. M. Lorilla, T. A. Keim, J. H. Lang, and D. J. Perreault, "Foil field lundell alternator with rotating power electronics," in *Proc. IEEE Power Electron. Spec. Conf.*, June 2006, pp. 1–6.

[28] E. Jung, S. Kim, J. Ha, and S. Sul, "Control of a synchronous motor with an inverter integrated rotor," *IEEE Trans. Ind. Appl.*, vol. 48, no. 6, pp. 1993–2001, Nov 2012.

[29] S. Choe, E. Jung, and S. Sul, "Sensorless control of synchronous machine with an inverter integrated rotor," *IEEE Trans. Ind. Appl.*, vol. 50, no. 4, pp. 2584–2591, July 2014.

[30] Z. Pang, M. Luvisotto, and D. Dzung, "Wireless high-performance communications: The challenges and opportunities of a new target," *IEEE Ind. Electron. Mag.*, vol. 11, no. 3, pp. 20–25, 2017.

[31] D. X. Llano, S. Abdi, M. Tatlow, E. Abdi, and R. A. McMahon, "Energy harvesting and wireless data transmission system for rotor instrumentation in electrical machines," *IET Power Electron.*, vol. 10, no. 11, pp. 1259–1267, 2017.

[32] T. Poller, T. Basler, M. Hernes, S. D?Arco, and J. Lutz, "Mechanical analysis of press-pack igbts," *Microelectron. Rel.*, vol. 52, no. 9-10, pp. 2397–2402, 2012.

[33] H. Oh, B. Han, P. McCluskey, C. Han, and B. D. Youn, "Physics-of-failure, condition monitoring, and prognostics of insulated gate bipolar transistor modules: A review," *IEEE Trans. Power Electron.*, vol. 30, no. 5, pp. 2413–2426, May 2015.

[34] R. Pittini, M. Hernes *et al.*, "Pressure-tolerant power electronics for deep and ultradeep water," *Oil&Gas fac.*, vol. 1, no. 01, pp. 47–52, 2012.

[35] K. Rajashekara and H. Krishnamoorthy, "Power electronics for subsea systems: Challenges and opportunities," in *Proc. IEEE Int. Conf. Power Electron. Drive Syst.*, Dec 2017, pp. 986–991.

[36] M. A. Kedzierski, R. Brignoli, K. Quine, and J. Brown, "Viscosity, density, and thermal conductivity of aluminum oxide and zinc oxide nanolubricants," *Int. J. Refrigeration*, vol. 74, pp. 1–9, 2017.

[37] I. E. T. Com., "Environmental testing–part 2-6: Test–test fc: Vibration (sinusoidal)," *Int. Std. CEI*, pp. 60 068–2.

[38] ——, "Fixed capacitors for use in electronic equipment–part 16-1: Blank detail specification: Fixed metallized polypropylene film dielectric d.c. capacitors - assessment levels E and EZ," *Int. Std. CEI*, pp. 60 384–16–1.

[39] G. Terzulli, "Evolution of power capacitors for electric vehicles," *Rep. KYOCERA group comp.*, 2012.

[40] S. Nuzzo, M. Galea, C. Gerada, and N. Brown, "Analysis, modeling, and design considerations for the excitation systems of synchronous generators," *IEEE Trans. Ind. Electron.*, vol. 65, no. 4, pp. 2996–3007, April 2018.

[41] J. K. Nøland, S. Nuzzo, A. Tessarolo, and E. F. Alves, "Excitation system technologies for wound-field synchronous machines: Survey of solutions and evolving trends," *IEEE Access*, vol. 7, pp. 109 699–109 718, 2019.

[42] J. K. Nøland, E. F. Alves, A. Pardini, and U. Lundin, "Unified reduced model for a dual-control scheme of the high-speed response brushless excitation system of synchronous generators," *IEEE Trans. Ind. Electron.*, vol. 67, no. 6, pp. 4474–4484, June 2020.

[43] F. Evestedt, *Improving the Functionality og Synchronous Machines using Power Electronics*. Lic. Eng., Div. Elect., Uppsala Univ., 2017.